Synthesis of Functional *Carbo*-benzenes with Functional Properties: The C_2 Tether Key

Kévin Cocq[a,b]
Cécile Barthes[a,b]
Arnaud Rives[a,b]
Valérie Maraval*[a,b]
Remi Chauvin*[a,b]

[a] CNRS, LCC (Laboratoire de Chimie de Coordination), 205 Route de Narbonne, BP44099, 31077 Toulouse Cedex 4, France
valerie.maraval@lcc-toulouse.fr
remi.chauvin@lcc-toulouse.fr
[b] Université de Toulouse, UPS, ICT-FR 2599, 31062 Toulouse Cedex 9, France

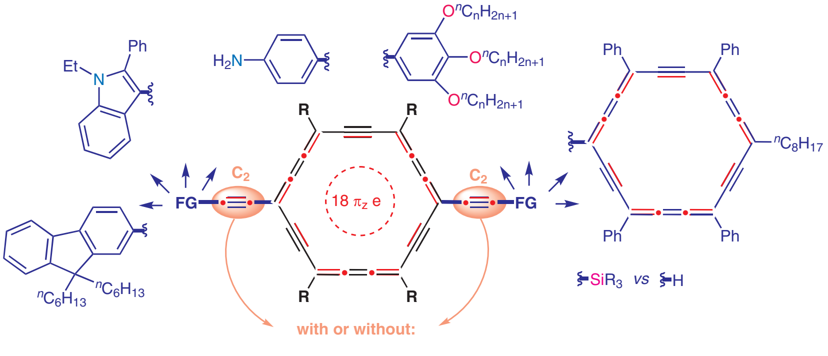

versatile effects on stability, solubility, magnetic anisotropy, molecular conductance, columnar mesogenicity, one-photon and two-photon absorption, π-cooperative surface photosensitization

Received: 11.07.2018
Accepted after revision: 13.08.2018

DOI: 10.1055/s-0037-1610269; Art ID: st-2018-a0437-a

Abstract Beyond demonstration of conceptual relevance and synthetic feasibility of aryl/alkyl-substituted representatives, *carbo*-benzene molecules started to gain prospects of broader impact through the emergence of alkynyl derivatives. This is first illustrated by examples of di- and hexaalkynyl-*carbo*-benzenes, a *carbo*-naphthalene, a *carbo*-biphenyl, and two *carbo*-terphenyls. A focus is then given to dialkynyl derivatives by reference to the peripherally C_2-extruded parents. In the centrosymmetric quadrupolar series, the C_2 expansion or ethynylogation effect is more particularly considered for 9*H*-fluoren-2-yl, tris(O-*n*-alkyl)pyrogallyl, indol-3-yl, 4-anilinyl, and tetraphenyl-*carbo*-phenyl substituents on the following respective properties: two-photon absorption, chemical stability, columnar mesogenicity, on-surface photoinduced charge separation *vs* single-molecule conductance, and reduction potential. Topical results and prospects of application are discussed on the basis of crystallographic, spectroscopic, and electrochemical analyses *vs* DFT-calculated nuclear and electronic structures. For the sake of the discussion consistency, complementary experimental and computational results are disclosed in the dianilinyl series. Overall, it is shown that combined advances in strategy, protocols, and substrate scope of acetylenic synthesis remain crucial for the development of yet poorly explored but promising types of molecular materials.

Key words alkyne, C_2 tether, *carbo*-benzene, *carbo*-mer, π-conjugation

1 Introduction

The acetylenic spC_2 unit is ubiquitous in the structures of organic materials with diverse optical, electrical, magnetic, or supramolecular properties. As a linker, the spC_2 unit indeed provides rigidity, minimal steric hindrance, and efficient π-conjugation (elliptic torus of doubly degenerated π-orbitals). It most often occurs between π-unsaturated functional groups, in particular aromatic moieties, as illustrated by the paradigm of oligo(phenylethynyl)enes (OPEs). This occurrence benefits from the general applicability of the Sonogashira sp^2C–spC coupling reaction. However, the C_∞-axial dicarbon unit is more than a linker and actually acts as an 'expander', preserving the local valence shell electron pair repulsion (VSEPR) geometrical relationships between the connected moieties. As formally proposed through the *carbo*-mer concept,[1a,b] the intrinsic C_2-expansion effect should be appraised by comparison of any acetylenic molecule with its parent where all the spC_2 units have been formally extruded.[1a] This would be topically illustrated by the ethynylogous series OPEs *vs* OPPs (oligo-*para*-phenylenes), but to the best of the authors' knowledge, literature lacks report of such systematic comparison for any particular property.[2] Though much less invoked than vinylogation, the ethynylogation process was, however, formally invoked in different contexts.[1d–h]

For now two decades, most efforts in *carbo*-mer chemistry have been devoted to ring *carbo*-mers of benzenic derivatives of type **1**, simply named *carbo*-benzenes (Figure 1).[1a–c] The first representatives were reported in 1995 by I. Ueda, Y. Kuwatani, *et al.*,[3] simultaneously with the general definition of *carbo*-merization,[1c] giving rise to expanded carbon- and π-electron-rich molecules, naturally calling for comparison with their nonexpanded parent, at least at the theoretical level.[4] In particular, the Hückel 4n+2 π-electron

Biographical Sketches

After few months in Prague, Czech Republic, working on Helicene chemistry under the supervision of Dr. Irena G. Stara, **Kévin Cocq** came back to Toulouse, France. He obtained his PhD in 2015 under the supervision of Prof. Remi Chauvin and Dr. Valérie Maraval at the Laboratoire de Chimie de Coordination (LCC). He worked on the synthesis of *carbo*-quinoids (expanded analogue of quinodimethane) and *carbo*-benzenoids (as small fragment of *α*-graphyne). He then spent ten months as a postdoctoral fellow for the synthesis of novel photosensitizers for water-splitting process. He is currently teacher at the Université Paul Sabatier in Toulouse, France and he carries on the development of catalysts for efficient water-splitting technology.

Cécile Barthes obtained a diploma of advanced technician in 2003 in synthesis chemistry. Then she worked in CEMES-CNRS for 2004–2007 on the synthesis of polyaromatic compounds under the supervision of Andre Gourdon. Then she worked six months at Sanofi-Aventis in the field of research synthesis. In late 2007 she joined LFHA for one year with industrial contract working on silicon polymers. Since 2008, she got a position in LCC-CNRS in 2008 as technician in chemical synthesis. She is taking part in various projects in syntheses forming electron-rich organics molecules as *carbo*-mers to phosphino-carbene complexes.

Arnaud Rives was born in 1981 in l'Union, France. He completed his PhD in 2010 at the SPCMIB laboratory in Toulouse under the supervision of Yves Génisson. After a two-year postdoctoral fellow stay at the 'Laboratoire de Chimie de Coordination' in Toulouse with Valérie Maraval and Remi Chauvin, he has joined the biotechnology company AFFICHEM in Toulouse since 2012, as chemistry laboratory manager.

Valérie Maraval obtained her PhD in 2000 under the supervision of Jean-Pierre Majoral in Toulouse, France. In 2001, she worked as a postdoctoral fellow with Bernard Meunier and the Aventis company. She then came back to Jean-Pierre Majoral's team as a CNRS engineer. In 2005, she joined the group of Remi Chauvin at the Laboratoire de Chimie de Coordination in Toulouse as a CNRS research engineer, where she completed her Habilitation in 2014. Her research activity focuses on two aspects of acetylenic chemistry: (i) synthesis of carbon-rich and electron-rich molecules (*carbo*-mers) for the study of their optical, electronic, and mesogenic properties; (ii) synthesis of biologically active chiral acetylenic lipids inspired from natural products.

Remi Chauvin, Professor at the Paul Sabatier University, has been leading his research at the Laboratoire de Chimie de Coordination of the CNRS in Toulouse since 1998. Before, he was successively PhD student with Prof. Henri Kagan in Orsay, France (1986–1988), postdoctoral fellow with Prof. Barry Sharpless in Cambridge, MA, USA (1989), then with Prof. Andrea Vasella in Zürich, Switzerland (1990), R&D investigator at the Roussel-Uclaf company in Romainville, France (1990–1993), and CNRS research associate in Toulouse (1993–1998). Since 2008 he is in charge of interuniversity relationships with research institutions in Ukraine and was awarded *Doctor Honoris Causa* of the Taras Chevtchenko National University in Kiev in 2015. Since 2015 he is recurrent invited professor at Huaqiao University, Xiamen, China, where he manages a research outpost at the School of Biomedical Sciences. Within the framework of relevant collaborations, his research interests extend from organometallic main group chemistry for catalysis (extreme phosphocarbon ligands) to mathematical-computational chemistry for theoretical analysis (quantification of chemical concepts, chirality, aromaticity, dativity), through organic chemistry for physics (*carbo*-meric molecules with optical, electrical or liquid crystal properties) and organic chemistry for biology (bioinspired lipidic acetylenic molecules with antitumor or antibacterial properties).

count of the C_{18} ring provides *carbo*-benzenes with a '*carbo*-aromatic' character[1b] underlying unique chromophoric, electric, or supramolecular properties, notably different from those of parent benzenes and nonaromatic π-conjugated counterparts such as *carbo*-butadienes **2**,[5] *carbo*-cyclohexadienes **3**,[6] or *carbo*-quinoids **4**.[1,7]

Carbo-benzenes have been mostly produced by reductive aromatization of hexaoxy[6]pericyclynes formed by heteropolar macrocyclization reactions characterized by patterns of the type [m + (18 – m)], where m denotes the number of carbon atoms of the target C_{18} ring brought by the nucleophilic reactant (m = 8, 9, 11, 14). [8] While the bare *carbo*-benzene $C_{18}H_6$ remains unknown (*a priori* because of the instability of envisaged synthetic intermediates),[9] only a few partially tetra- or trisubstituted versions have been reported,[3,10] all the other representatives being hexasubstituted, of generic formula $C_{18}R^1R^2R^3R^4R^5R^6$, $R^i \neq H$. Beside recent examples of alkyl substitution (R^i = *n*-C_nH_{2n+1}, $2 \leq n \leq 20$, ***i***-Pr, ***t***-Bu),[11] most of the known *carbo*-benzenes bear aromatic groups (R^i = 4-X-C_6H_4, pyrogallyl, indolyl, fluorenyl, ...), and less frequently alkynyl groups R^i = $-C{\equiv}C-R'^{i}$.[1,10a,12] Beyond their postfunctionalization potential, the latter are, however, basically attractive for the above-emphasized 'pure' expander effect of the *sp*C_2 unit.

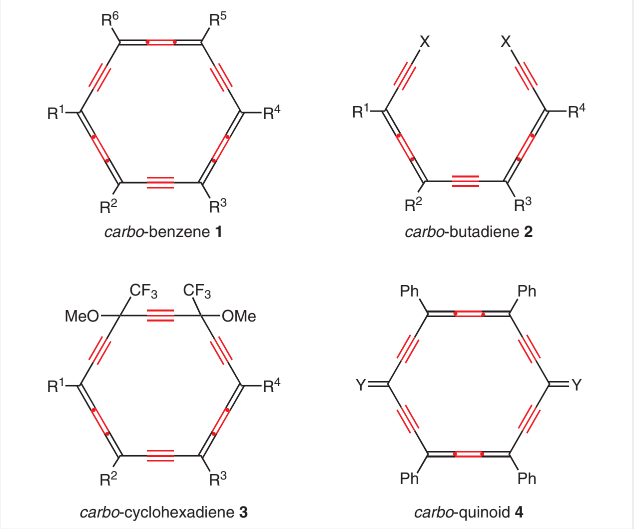

carbo-benzene **1**

carbo-butadiene **2**

carbo-cyclohexadiene **3**

carbo-quinoid **4**

Figure 1 Main prototypes of *carbo*-mer molecules with extended π-conjugation

Alkynyl-substituted *carbo*-benzenes are thus surveyed hereafter from both the standpoints of properties and synthesis. Except the hexaalkynyl representative **1a**,[12] all other know examples are tetraarylated with two alkynyl substituents only.

2 Hexaalkynyl-*carbo*-benzene

With six triethylsilylethynyl groups, **1a** can be considered as a Si-protected version of the total *carbo*-mer of benzene $C_{18}(C_2H)_6$,[12] completing the features of the peripheral counterpart, hexaethynylbenzene,[13a] among other perethynyl [n]annulene derivatives $C_n(C_2R)_n$, n = 3–5, 8.[13b–p] The target **1a** was prepared through a 16-step sequence involving a [8+10] macrocyclization step from the C_8-pentayne **5a** and the C_{10}-diketone **6** (Scheme 1). Reductive aromatization of the resulting hexaalkynylated [6]pericyclynediol **7** could not be performed under the standard conditions used for the aromatization of arylated counterparts, *i.e.*, by treatment with $SnCl_2$ and HCl.[1,3a] This was attributed to the destabilization of the six equivalent putative trialkynyl carbenium primary intermediates: In the absence of steric hindrance to planar π-C^+ conjugation, a propargylic C–OR bond is indeed less prone to heterolytic dissociation than benzylic counterparts.[14] Stabilization of the carbenium centers was thus envisaged via Nicholas' complexes generated *in situ* by treatment of **7** with two equivalents of $Co_2(CO)_8$:[15] The anticipated complexes **7**·$Co_2(CO)_6$ or **7**·$[Co_2(CO)_6]_2$ were not isolated, but treatment with $SnCl_2$/HCl, followed by oxidative Co-decoordination with ceric ammonium nitrate, afforded **1a** with 12% yield over three steps in one pot.[12] While the six $SiEt_3$ groups surrounding the rigid C_{30} core provided sufficient solubility for full characterization of **1a** (including by ^{13}C NMR spectroscopy), attempts at protodesilylation resulted in the deposit of a black solid, which was not characterized but tentatively attributed to the extremely carbon-rich stoichiometry $C_{30}H_6$ (C/H = 5, equivalent to that of the [4]coronene graphene flake $C_{150}H_{30}$ made of 61 C_6 hexagons).[16] The total *carbo*-mer of benzene $C_{18}(C_2H)_6$ thus remains uncharacterized experimentally, but was studied in detail at the DFT computational level (B3PW91/6-31G(d,p)), and compared with the corresponding ring *carbo*-mer $C_{18}H_6$.[4d] The effect of C_2-tethering of six H atoms to the C_{18} core happens to be limited: both the root-mean-square deviation from the mean C–C bond length (σ_r) and nucleus-independent chemical shift at the center of the ring (NICS) increase slightly from $\sigma_r = 0.061$ Å and NICS = –19.7 ppm for $C_{18}H_6$ to $\sigma_r = 0.070$ Å and NICS = –17.8 ppm for $C_{18}(C_2H)_6$. These variations reveal a slight loss of the aromatic character of the C_{18} ring according to structural and magnetic criteria, indeed anticipated to be induced by π-conjugation extension over 12 external *sp*C atoms. The same trend was recently observed in a series of *tert*-butyl-substituted *carbo*-benzenes, $C_{18}Ph_n tBu_{6-n}$, in which magnetic anisotropy was shown to decrease upon increasing the number n of phenyl substituents.[11d]

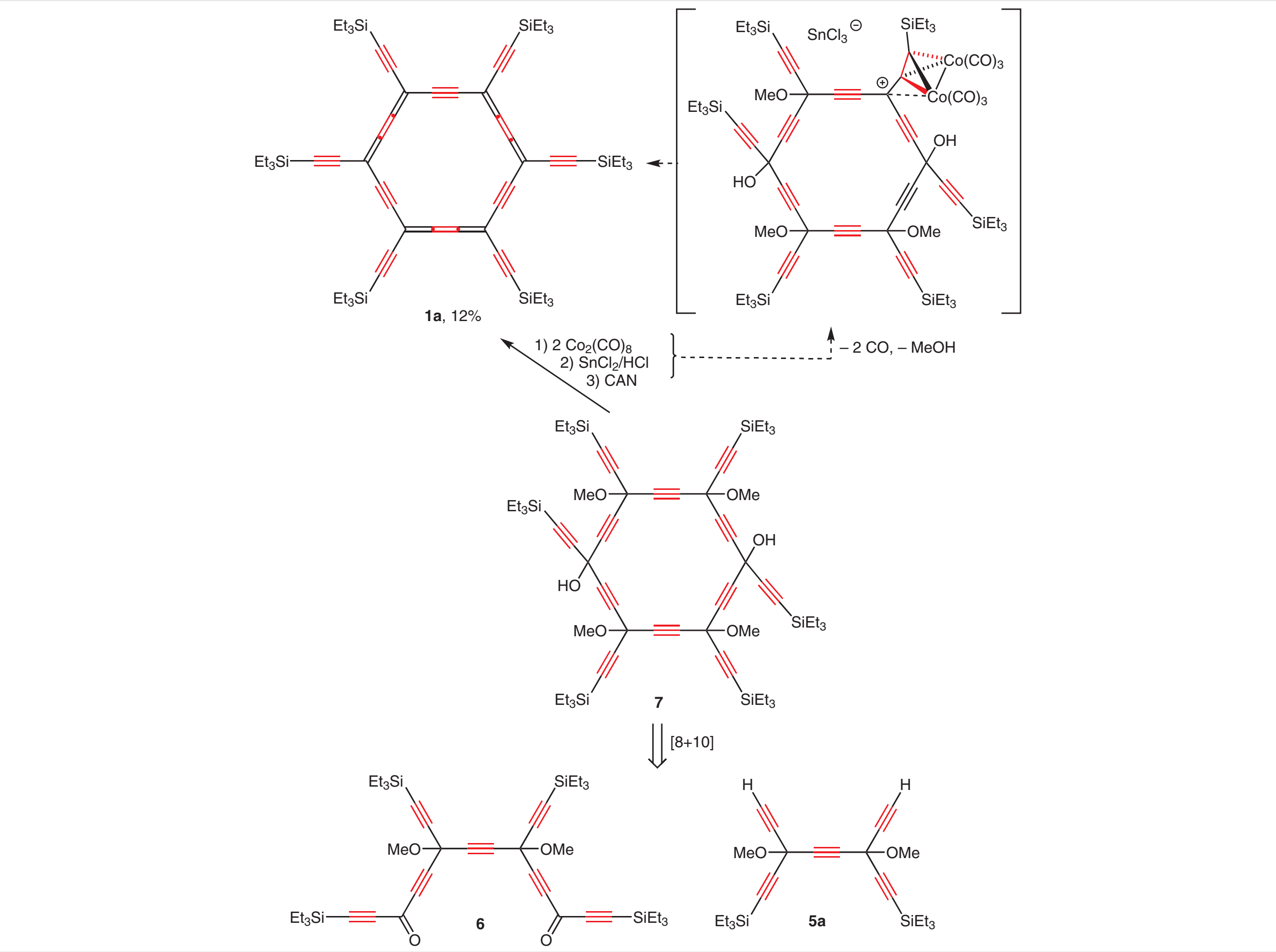

Scheme 1 Synthesis of the hexaalkynyl-*carbo*-benzene **1a**

3 *ortho*-Dialkynyl-*carbo*-benzenes

One example of *ortho*-dialkynyl-*carbo*-benzene, **1b**, was recently described within the context of the synthesis of the *carbo*-naphthalene **8** relying on the dialkynyl-[6]pericyclynediol intermediate **9** (Scheme 2).[17] The latter, obtained by [8+10] macrocyclization from the pentayne **5b** and diketone **10**, was thus independently submitted to the reductive aromatization reagent $SnCl_2$/HCl, producing **1b** with 16% yield. Noteworthy is the formal *ortho*-dialkynyl-*carbo*-benzenic character **8A** of the *carbo*-naphthalene **8** itself, albeit diluted in the Kekulé resonance with the *ortho*-*carbo*-quinoid forms **8B**, featuring a 1,16-bridged *carbo*-[10]annulene.

4 *para*-Dialkynyl-*carbo*-benzenes

Most of the dialkynyl-*carbo*-benzenes exemplified hitherto belong to the *para* series, *i.e.*, with two alkynyl substituents at the 1,10-positions of the macrocycle. This is mainly due to versatility of a general synthetic route involving a pivotal [6]pericyclynedione synthon (see section 4.1 and Scheme 3).

4.1 *Bistrimethylsilylethynyl-carbo-benzene*

The bistrimethylsilylethynyl-*carbo*-benzene **1c** was accessed through two alternative [14+4] and [8+10] macrocyclization processes (Scheme 3).[18,10a] The [14+4] route involved the C_{14}-dinucleophile **11** and C_4-dielectrophile **12**,[19] the former being obtained in four steps from the dialdehyde **13**, itself prepared in five steps from commercial materials.[18]

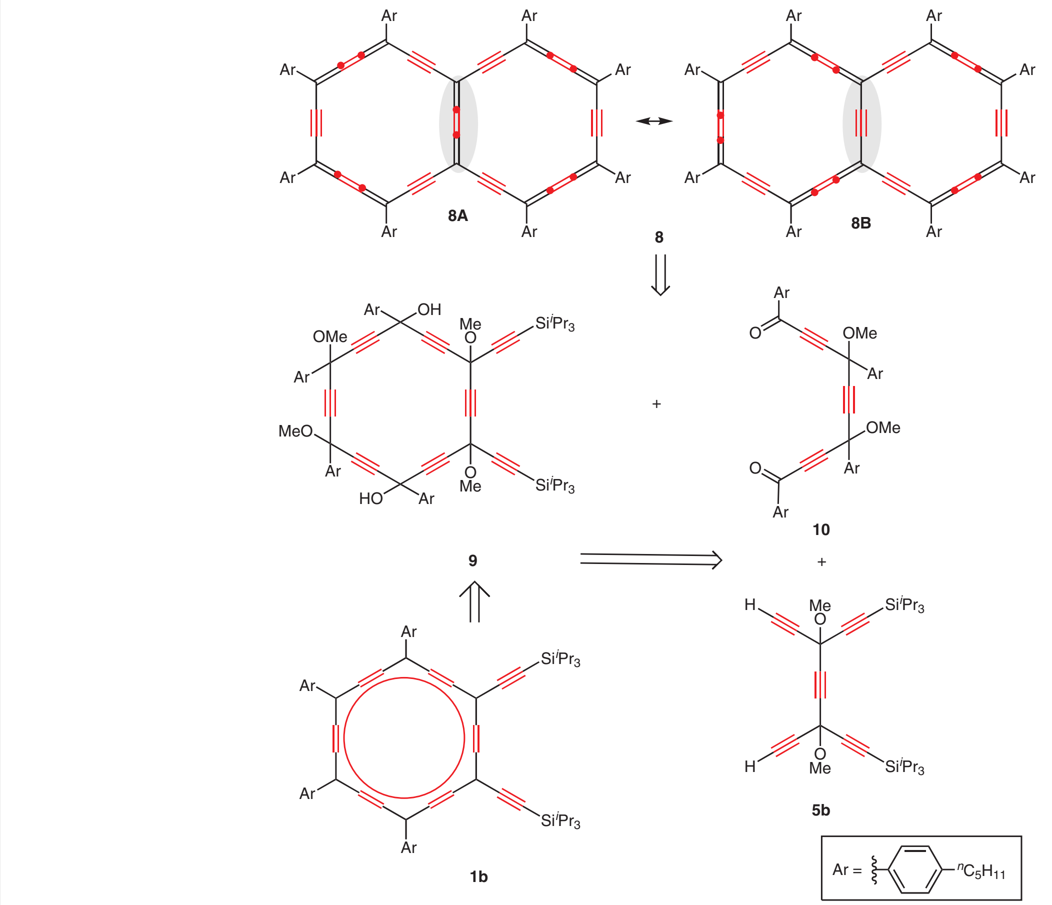

Scheme 2 Synthesis of the *ortho*-dialkynyl-*carbo*-benzene **1b** and *carbo*-naphthalene **8**

Addition of the dilithium salt of **11** to dibenzoylacetylene **12** afforded the [6]pericyclynediol **14a** with 43% yield. Subsequent reductive aromatization with $SnCl_2$/HCl afforded **1c** with 10% yield.

This 13-step synthesis of **1c** was later superseded by a [8+10] route regarded as optimal for symmetrical *para*-disubstituted *carbo*-benzene targets.[8d] The strategic efficiency is here due to both the selectivity of the cyclization process and its late divergent character, the C_{10}-dielectrophile **13** being directly prepared from the C_8-dinucleophile **15**. The [6]pericyclynedione intermediate **16** is also a versatile precursor to which various nucleophiles can be added, thus allowing a two-step access to a wide range of *para*-disubstituted *carbo*-benzenes.[8d] Addition of the dimagnesium salt of **15** to **13** thus led to the [6]pericyclynediol **17**, which was then oxidized to the diketone **16** with MnO_2 (Scheme 3). Addition of trimethylsilylethynyl-magnesium bromide to **16** gave **14b** with an unoptimized yield of 17%. Ultimate reductive aromatization of **14b** gave access to **1c** in 12 steps. Though attempts at isolating the deprotected diethynyl-*carbo*-benzene **1d** failed, a signal at $\delta = 4.3$ ppm in the ^{1}H NMR spectrum of a soluble extract from the black material product could be assigned to the terminal acetylenic proton of **1d**,[10a] the C_2-extruded version of which (H-$C_{18}Ph_4$-H) has been described in detail.[10] Nevertheless, the C_2-extruded version of **1c**, *i.e.*, $Me_3Si–C_{18}Ph_4–SiMe_3$, with two C_{18}–heteroatom bonds, is still missing and definitely deserves future synthesis efforts.

4.2 *Bisfluorenylethynyl-carbo-benzene*

Fluorophore-substituted *carbo*-benzenes were targeted with the aim of studying their nonlinear optical (NLO) properties, in particular their two-photon absorption (TPA) efficiency, a 3^d-order NLO property. On the basis of numerous examples, quadrupolar extended π-conjugated systems have indeed been proposed as systematic TPA chromophore candidates.[20] Fluorenyl moieties, widely used as weakly donor ends D in D–Π–D TPA systems centered on a π-conjugated core Π,[21] were thus also envisaged for a *carbo*-*p*-phenylene Π core. Two *carbo*-benzenes, **1e** and **1f**, differing by the fluorenyl–C_{18} tethering mode, were thus prepared in two steps from the key [6]pericyclynedione **16** (Scheme 4).[22] Reaction of **16** with dihexylfluorenyllithium **18a** and

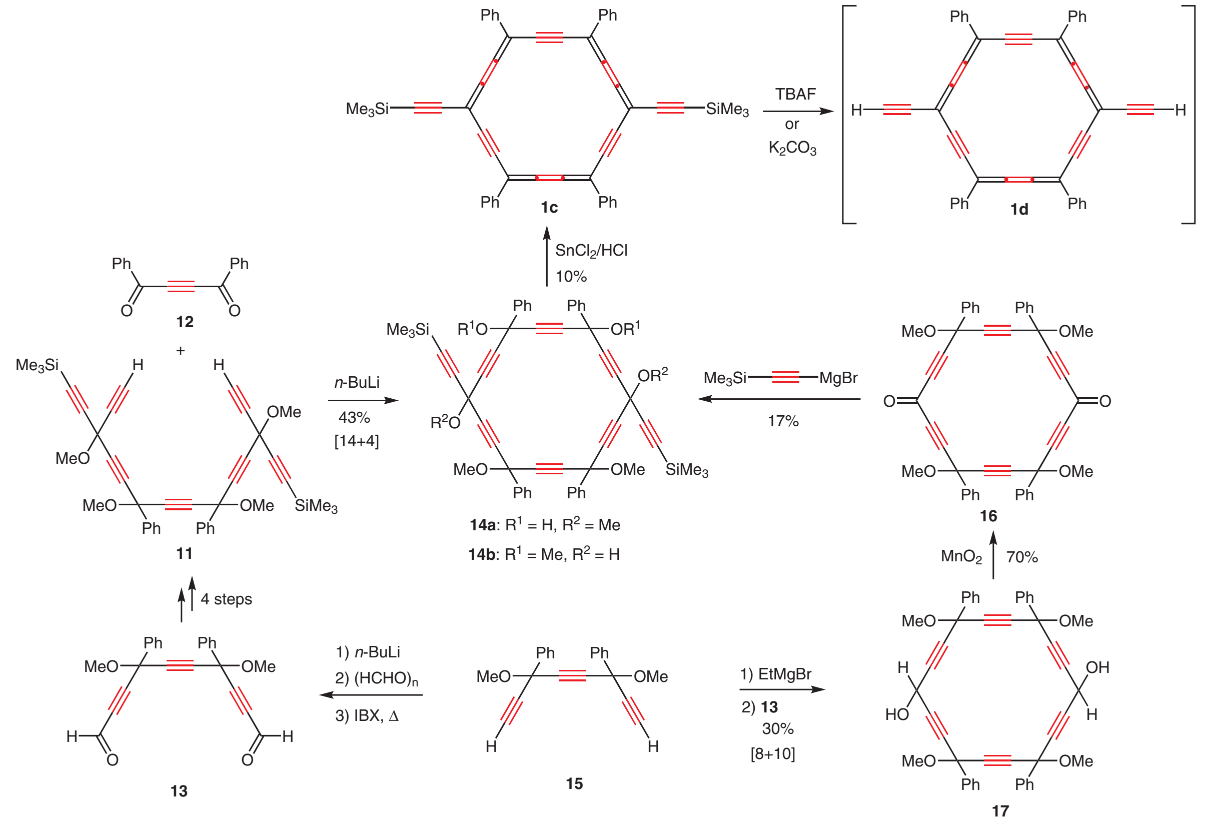

Scheme 3 Alternative strategies for the synthesis of the bistrimethylsilylethynyl-tetraphenyl-*carbo*-benzene **1c**

dihexylfluorenylethynyl-magnesium bromide **18b** thus gave the pericyclynediols **19a** and **19b** in 41% and 50 % yield, respectively. Subsequent reductive aromatization with $SnCl_2$/HCl afforded the target *carbo*-benzenes **1e** and **1f** in 55 ± 4% yield.

Insertion of ethyndiyl expanders between the *carbo*-benzene core and fluorenyl groups of **1e** was found to have a dramatic effect on TPA, with a negligible effect on one-photon absorption (OPA; the maximum absorption wavelengths remaining at 493 ± 1 nm in **1e** and **1f**, their extinction coefficient being also comparable at 355 000 ± 25 000 L mol^{-1} cm^{-1}, the highest ε value being obtained for **1f**).[22]

The TPEF method being prevented by a very weak fluorescence, the use of the z-scan method with femtosecond excitation at 800 nm showed that the TPA cross-section of **1e** (σ_{TPA}= 336 GM) is notably increased in **1f**, reaching 656 GM.[22] On the basis of TDDFT-calculated one-photon- and two-photon-allowed excited states reproducing experimental values, the twofold enhancement factor of σ_{TPA} from **1e** to **1f** estimated by the sum-over-state (SOS) approach is mainly due to the increase of the first transition dipole moment of the intermediate OPA transitions (contributing to 81% of the overall σ_{TPA}value).

Double ethynylogation has also a significant effect on the first reduction and oxidation potential values, changing from –0.75 V and +1.08 V/SCE in **1e** to –0.61 V and +1.17 V/SCE in **1f**. Notably, $E^{red}_{1/2}$ (**1f**) = –0.61 V is the highest reduction potential value reported to date for a mono-*carbo*-benzene derivative.

4.3 *Bistrialkoxyarylethynyl-carbo-benzenes*

Carbo-benzenes attached to pyrogallol *n*-alkyl ether groups were recently targeted with the aim of investigating the ability of the flat, flexible, and empty *carbo*-aromatic C_{18} ring[1b] to act as a discotic mesogenic core of 'hollow columnar' liquid crystals.[23] The synthesis of **1g**, where the C_{18} ring is directly substituted by *O,O′,O″*-trisoctadecyl-pyrogallyl groups failed, due to the difficulty to generate the bromomagnesium reagent from **20a** required for the preparation of the pericyclynediol precursor **21a**.[24] However, recourse to two *sp*C_2 tethers allowed access to **1h** and **1i** bearing pyrogallylethynyl groups.[25] The ethynylpyrogallol triethers **22a** and **22b**, differing by the length of the six *n*-alkyl chains C_nH_{2n+1} (**22a**: n = 18, **22b**: n = 12), were prepared following known procedures,[26] and their lithium or bromomagnesium salt added to the [6]pericyclynedione **16** to give

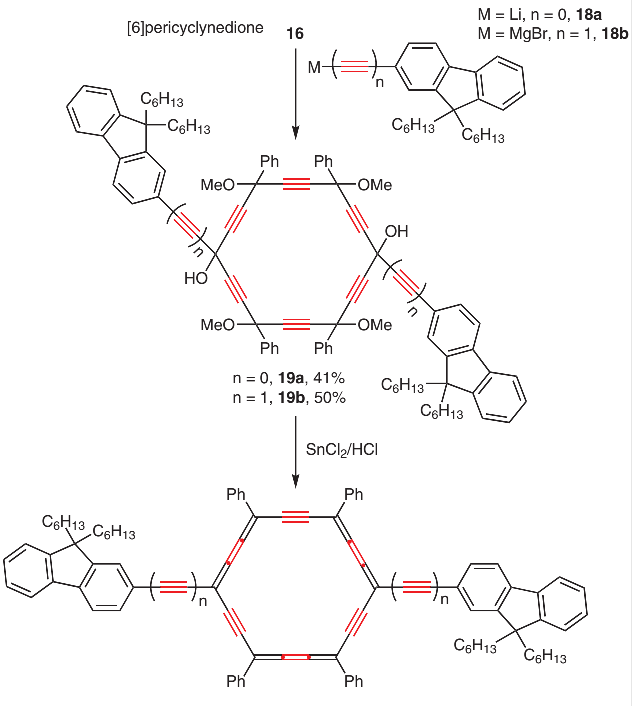

n = 0, **1e**, 59%, λ_{max} = 492 nm, σ_{TPA} (800 nm) = 336 GM (calcd. 227 GM; μ_{0i} = 1.7 au)
n = 1, **1f**, 51%, λ_{max} = 494 nm, σ_{TPA} (800 nm) = 656 GM (calcd. 349 GM; μ_{0i} = 2.4 au)

Scheme 4 Synthesis of fluorenyl-*carbo*-benzenes **1e** and **1f**, and TPA cross-section measured by the z-scan method or estimated by the SOS approach using excited states calculated at the TD-CAM-B3LYP/6-31G** level. μ_{0i}= transition dipole moment from the ground state to the main intermediate one-photon-allowed excited state contributing the overall σ_{TPA}value.

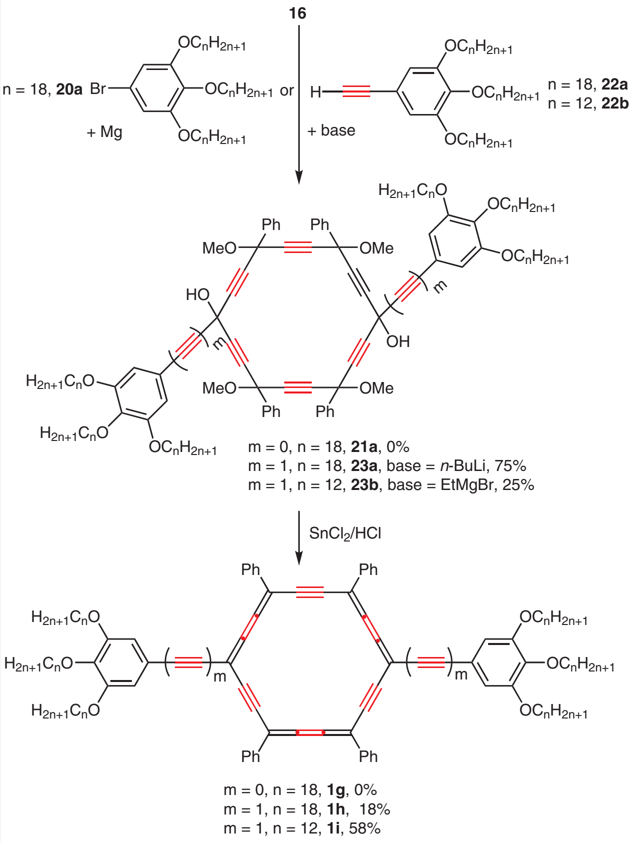

Scheme 5 Synthesis of *carbo*-benzenic mesogens

the respective pericyclynediols **23a** and **23b**. After reductive aromatization, the *carbo*-benzenes **1h** and **1i** were isolated in 18% and 58% yield, respectively (Scheme 5).

As **1i** was found to be more soluble and available in larger amounts than **1h**, its ability to give liquid crystalline mesophases was investigated in a systematic manner using powder X-ray diffraction (PXRD), polarized optical microscopy (POM), and differential scanning calorimetry (DSC). All the analytical data confirmed the formation of a columnar rectangular mesophase at 115 °C. STM images of the 2D self-assembly of the '*carbo*-mesogen' **1i** on a HOPG surface also evidenced a rectangular arrangement (48 × 43 Å^2) comparable to the axial projection of the 3D columnar assembly (48.5 × 45 Å^2, Figure 2, a and b).[25] In the crystal state, the packing is monoclinic (prismatic $P2_1/c$ space group), *i.e.*, also truly rectangular with a long cell axis, of length a = 49.45 Å, close to the PXRD or STM values and to the diameter of the molecular skeleton (51.3 Å). Noteworthy is the absence of direct π–π stacking between C_{18} rings forming hexagonal columns parallel to the crystallographic c axis, slanted by 17.4° with respect to the normal of the constituting parallel C_{18} mean planes separated by a 7.02 Å increment (Figure 2, c): Two phenyl rings pointing from neighboring columns indeed intercalate between two successive C_{18} rings (with shortest C···C distances of 3.44 Å between the two C_6 rings, 3.41 Å between the C_{18} and C_6 rings). The neighboring columns also interact by weak π–π stacking of pyrogallol C_6 rings (3.42 Å), itself driven by dispersive interaction between the respective triads of parallel stretched $C_{12}H_{25}$ chains. Interdigitation of dodecyl chains, also evidenced in STM images, is thus assumed to occur in the discotic mesophase, where neighboring columns interpenetrate by intercalation of C_6 rings within channels of C_{18} rings.

The discotic mesogenic properties of **1i** rely first on its spontaneous ability to adopt a near-planar structure in the condensed phase (in the crystal, the maximum distance from a C or O atom to the molecular mean plane is 2.3 Å, for a diameter of 51.3 Å). This minimal strain can be directly attributed to the spC_2 expander allowing minimal steric repulsion between the trialkoxyaryl moieties and the $C_{18}Ph_4$ core.

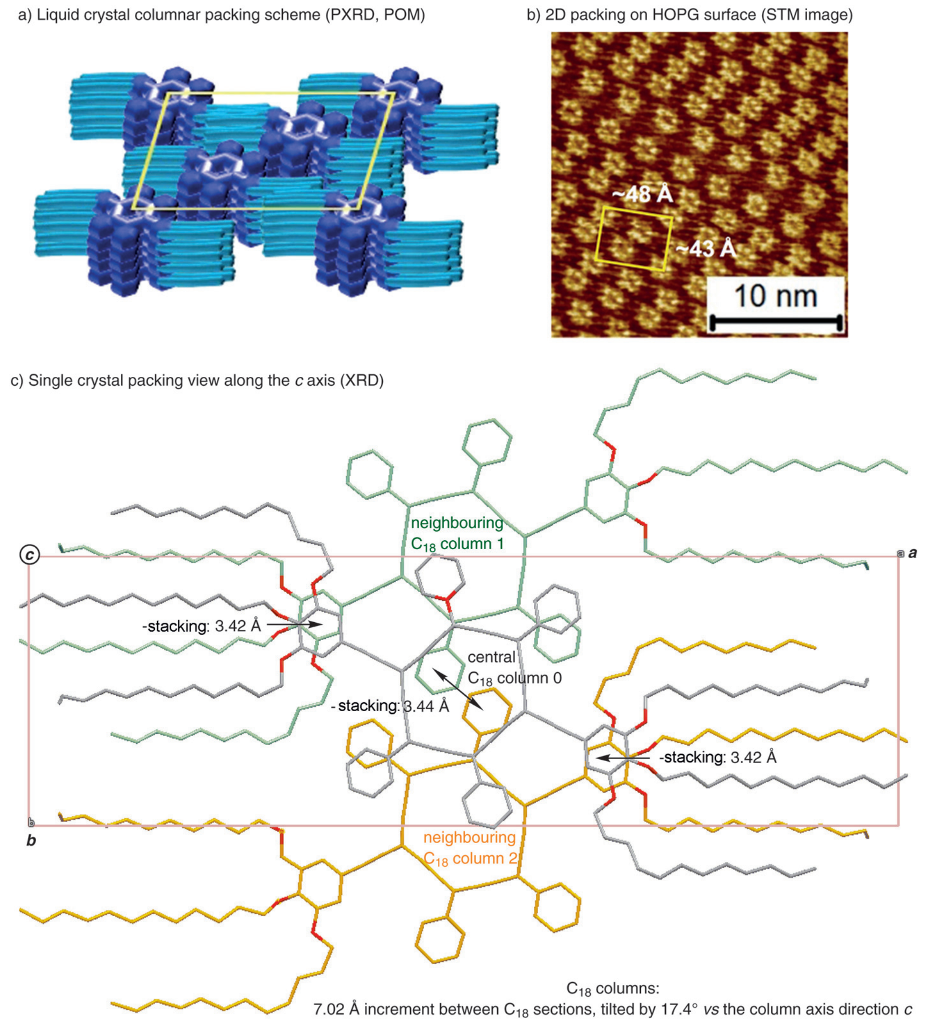
a) Liquid crystal columnar packing scheme (PXRD, POM)

b) 2D packing on HOPG surface (STM image)

c) Single crystal packing view along the *c* axis (XRD)

C_{18} columns:
7.02 Å increment between C_{18} sections, tilted by 17.4° *vs* the column axis direction *c*

Figure 2 a) Cartoon representation of the rectangular columnar 3D packing of *carbo*-mesogen **1i**; b) STM image showing the rectangular 2D arrangement of **1i** over an HOPG (highly oriented pyrolytic graphite) surface; c) single-crystal packing of **1i**, view along the C_{18} column direction, corresponding to the crystallographic axis *c* (= 7.35 Å; *b* = 15.29 Å, *a* = 49.45 Å; $P2_1/c$ space group).

4.4 *Bisindolyl(ethynyl)-carbo-benzene*

With the view to outlining prospects of electrooptical applications of *carbo*-benzene derivatives (SMC, NLO, TPA, OPV, ...), the effect of substitution on both the UV-visible absorption and redox behavior was considered for various types of nitrogen-containing π-donating groups. In a series of 4-anilinyl derivatives, where the N atom is thus connected to the C_{18} ring through an aromatic, so somewhat π-insulating, 1,4-phenylene spacer, a bathochromic shift of the maximum absorption was observed upon increasing the donating character (NMe_2 > NH_2 > indol-1-yl > carbazol-1-yl).[27] A more π-conducting N···C_{18} π-junction was then envisaged in the indol-3-yl- and indol-3-ylethynyl- *carbo*-benzenes **1j** and **1k**.[28] Their synthesis was tackled by the classical two-step process from the [6]pericyclynedione **16** and either the bromoindole **24** or ethynylindole **25** (Scheme 6).[28,29] Direct anchoring was performed from **24** by bromine–lithium exchange and addition to **16**, followed by reduction with $SnCl_2$/HCl. The diindolyl-*carbo*-benzene **1j** was thus isolated with 3% yield from **16**. X-ray diffraction analysis of single crystals of **1j** evidenced a limiting π-conjugation between the indole and *carbo*-benzene π-systems due to steric repulsion (dihedral angle: *sp*C–C–C–CN = 30.0°).

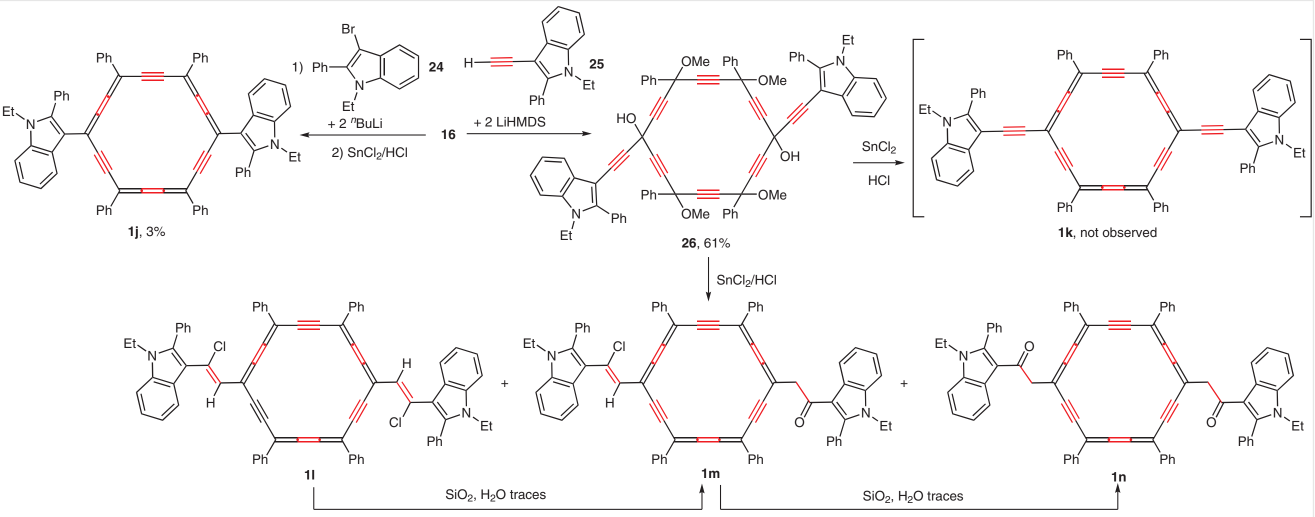

Scheme 6 Synthesis of indolyl-substituted *carbo*-benzenes

Targeting the indol-3-ylethynyl-*carbo*-benzene **1k**, the [6]pericyclynediol **26** was prepared in 61% yield by addition of **25** to the diketone **16** in the presence of LiHMDS. Subsequent treatment of **26** with SnCl$_2$/HCl, however, did not allow isolation of **1k**, but, instead, produced a mixture of three chromophores, among which the dialkenyl-*carbo*-benzene **1l** was the main product. Its formation resulted from a regio- and stereoselective addition of HCl onto the two external triple bonds of **1k**. This peculiar reactivity at room temperature was attributed to promotion by the combined effects of the adjacent π-electron-rich C_{18} ring and π-donating enamine group, inducing 'π-frustration' of the triple bonds. The dialkenyl-*carbo*-benzene **1l** was found to react with traces of water on silica gel to give the 2-oxoalkyl-*carbo*-benzenes **1m** and **1n** resulting from the hydrolysis of one or two chloroalkenyl units of **1l**, respectively (Scheme 6).[28] The propensity of the chloroalkene groups of **1l** to give the corresponding methylene ketones (or enol forms) is unusual, as such transformations generally require harsher acidic conditions.[30] This observation can also be ascribed to the double bond 'π-frustration' induced by the π-donating character of the enamine substituent facing the π-electron-rich *carbo*-benzene core.

4.5 *Bisanilinylethynyl-carbo-benzene*

The *para*-dianilinyl-*carbo*-benzene **1o** and diethynylogue **1p** were prepared by the classical two-step method from the [6]pericyclynedione **16** (Scheme 7). The synthesis of **1o** required the reaction of **16** with two equivalents of the Grignard reagent of *N*,*N*-bistrimethylsilyl-4-bromoaniline (**27a**). The resulting [6]pericyclynediol **28a** was, however, found to be unstable upon attempt at purification by column chromatography.[27] The crude material was thus directly treated with SnCl$_2$/HCl, then with NaOH, to deliver the reduced protodesilylated target **1o** with 26% yield from **16**.

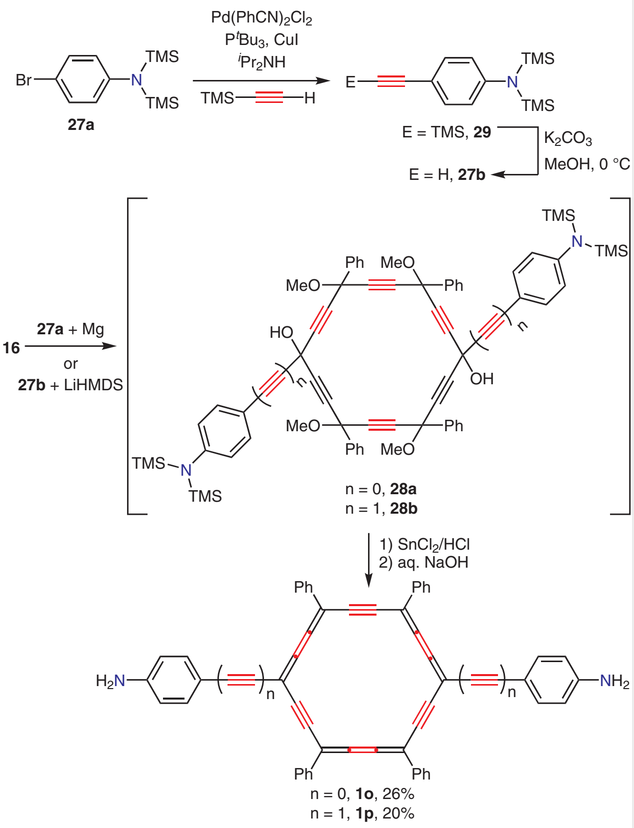

Scheme 7 Synthesis of the anilinyl(ethynyl)-*carbo*-benzenes **1o** and **1p** (the preparation and characterization of **27b** and **1p** are described in ref. 31 and 32).

Likewise, *N*,*N*-bistrimethylsilyl-4-ethynylaniline (**27b**) was required for the synthesis of **1p**. It was prepared in two steps from **27a**, the latter being first submitted to Sonogashira coupling with trimethylsilylacetylene to give the primary product **29**. Careful optimization of the reaction conditions allowed selective C-desilylation of **29** with K_2CO_3/MeOH, while avoiding N-desilylation (Scheme 7).[31] Addition of **27b** to **16** afforded the unstable pericyclynediol **28b**, which was directly treated with $SnCl_2$/HCl, then with aqueous NaOH, to give **1p** with 20% yield from **16**.[32]

As previously evidenced for fluorenylethynyl-*carbo*-benzenes (**1e** and **1f**, see section 4.2.),[22] **1o** and **1p** were found to display almost superimposable UV-vis spectra, with exactly the same maximum absorption wavelength at 493 nm, thus confirming the negligible effect of C_2-tethering on OPA.[27,32] As in the fluorenyl(ethynyl) series, C_2 tethering was found to induce a slight increase of the extinction coefficient (ε = 131 000 L mol^{-1} cm^{-1} for **1p** *vs* 105 000 L mol^{-1} cm^{-1} for **1o**). Notably, however, increase of the π-conjugation extent from **1o** to **1p** proved to have a significant effect on the redox properties, **1p** being both easier to reduce by 0.14 V and more difficult to oxidize by 0.16 V than **1o**.[32] A similar shift of the first redox potentials was observed in the fluorenyl series, **1f** being easier to reduce by 0.14 V and more difficult to oxidize by 0.09 V than **1e** (see Scheme 4 and section 4.2).[22]

The dianilinyl-*carbo*-benzene **1o** is also a highly efficient molecular conductor, with an unprecedented single-molecule conductance (SMC) as determined by the STM break junction method:[33] SMC(**1o**) = 106 nS over 2 nm (N···N distance measured by X-ray diffraction of a single crystal). This SMC value, much higher than those measured for other dianilinyl derivatives with similar N···N distances, highlights the *carbo*-benzene core as an attractive motif for the design of carbon-rich molecular device ruled by the spatial extent and quantum efficiency of π-electronic communication/excitation (mixed valence complexes, photovoltaic cells, light-emitting diodes, tunneling diodes, field-effect transistors, or any organic-semiconductor-based system).

With a 5.0 Å longer N···N distance, the SMC of **1p** is anticipated to be lower than that of **1o** and has not been experimentally determined yet.[34] The di(anilinylethynyl)-*carbo*-benzene **1p** was, however, recently shown to act as photosensitizer in a multicomponent nanocatalytic system for the production of dihydrogen by formal water splitting under solar irradiation (H_2O + red –[cat][$h\nu$]–> H_2 + redO).[35] According to SEM and TEM imaging, the core of the [cat] system, constituted by Ag plasmonic nanoparticles deposited on TiO_2 particles, is wrapped by a layer of **1p**. Speculatively, the latter might be a source of excitons expanding throughout the TiO_2 network to provide electrons for remote reduction of water molecules. A lower solubility/processability prevents the use of the nonexpanded counterpart **1o** as an alternative photosensitizer. Nevertheless, salient electronic effects of the ethynylogation of **1o** to **1p** are the anodic shift by 0.15 V, up to –0.67 V/SCE for the reduction of **1p** (and to +0.74 V for oxidation), and polarization of the HOMO→LUMO transition along the N···N direction (*x* axis): While the LUMO spreads out over the phenyl substituents (*y* axis) in **1o**, it expands over the C_2 tethers and anilinyl ends in **1p** (see Figure 3 and Supporting Information). This polarization is also apparent from the corresponding components of the traceless quadrupole moment (Q_{xx} = 146.0 D.Å and Q_{yy} = -23.8 D.Å for **1o**, Q_{xx} = 189.2 D.Å and Q_{yy} = –33.8 D.Å for **1p**) with a difference in quadrupolar dissymmetry $\Delta(Q_{xx} - Q_{yy})$ = 53.2 D.Å.

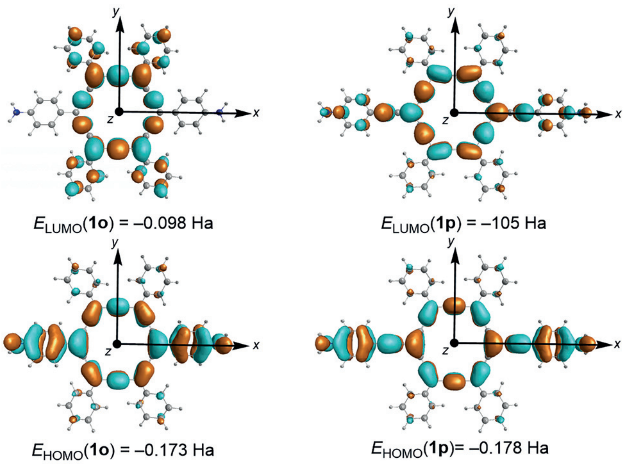

Figure 3 Frontier orbitals of the bisanilinyl-*carbo*-benzene **1o** and bisethynylogue **1p**. Optimized structures at the B3PW91/6-31G(d,p) level of calculation (D_2 symmetry for **1o**, C_i symmetry for **1p**); see Supporting Information.

5 *Carbo*-oligo(phenyleneethynylene)s

Skeletal *carbo*-mers of OPPs or ring *carbo*-mers of OPEs, containing several *carbo*-benzene rings connected by ethyndiyl linkers, were recently considered under the designation (ring) '*carbo*-OPEs' (Figure 4).[36] For practical synthesis reasons, aryl-substituted derivatives had to be targeted, and by virtue of the steric repulsion between facing phenyl substituents in the parent ring *carbo*-PPPs (e.g., *p*,*p*'-R–$C_{18}Ph_4$–$C_{18}Ph_4$–R), more efficient π-conjugation between C_{18} rings was indeed expected to occur in the *carbo*-OPE series (e.g., *p*,*p*'-R–$C_{18}Ph_4$–C≡C–$C_{18}Ph_4$–R). Concomitant effects of the π-overlap and intrinsic conductance of the C_{18} rings (see section 4.5) could indeed provide such molecular wires with remarkable electr(on)ical properties.[37] The synthesis of the three *carbo*-OPEs **1q**, **1r**, and **1s** was thus tackled by methods previously implemented for the preparation of dissymmetrically substituted *carbo*-benzenes (Scheme 8).[11c] The dissymmetrical precursors **29** and **30** were thus obtained from the [6]pericyclynedione **16** (Scheme 8).[36] Addition of lithiated **29** to the monoketone **30** and diketone **16** or **32** gave the bispericyclynediol **31** and trispericyclynediol **33** or **34**, respectively. Ultimate reductive aromatization furnished the *carbo*-biphenyl **1q** from **31**, and *carbo*-terphenyls **1r** and **1s** from **33** and **34**, respectively, with 9–20% yield from **29** (Scheme 8).[36]

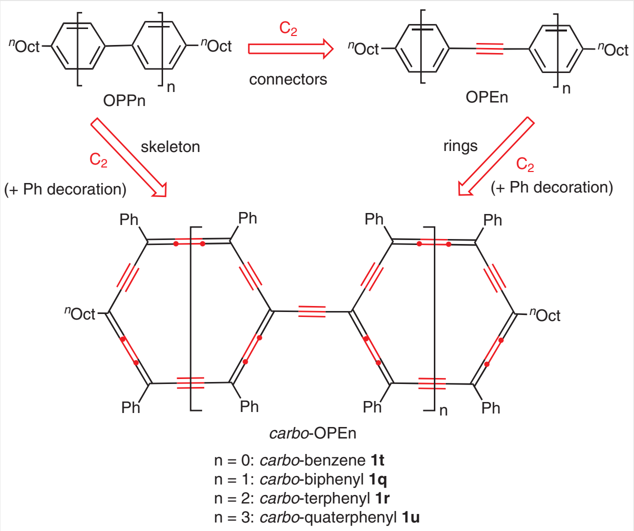

Figure 4 Design of *carbo*-OPEs, as ring *carbo*-mers of OPEs or skeletal *carbo*-mers of OPPs

The *carbo*-OPEs were obtained as dark-red solids stable at room temperature. As anticipated, the tetrapentylphenyl *carbo*-terphenyl **1s** proved to be significantly more soluble than the all-phenyl counterpart **1r**.

The UV-vis spectra of **1r** and **1s** exhibit three main absorption bands covering all the visible window, up to 750 nm. The π-conjugation extent is also revealed by very low absolute values of the first reversible reduction potentials, at –0.39 and –0.45 V/SCE for **1r** and **1s**, respectively. In a consistent manner, the *carbo*-biphenyl **1q** and *p*-dioctyl-*carbo*-benzene reference **1t** are reduced at lower potentials, –0.58 and –0.83 V/SCE, respectively.[11c] An accurate correlation of the reduction potential with the LUMO energy allows extrapolation to –0.30 V/SCE for the DFT-calculated *carbo*-quaterphenyl **1u** (Figure 4). This trend indicates the efficiency of conjugation between the $C_{18}Ar_4$ units, enabled by a low rotation barrier about the C_2 tethers (3 kcal mol^{-1}, fictitious nonarylated *carbo*-OPEs constituted by $C_{18}H_4$ units being even planar in the equilibrium ground state). This trend is to be related with the moderate energetic aromaticity of the C_{18} macrocycles,[4f] which, however, preserve a strong magnetic aromaticity. A strong diatropic ring current[4d] is indeed revealed by anisotropic NMR effects on the *ortho*-^{1}H nuclei of the aryl substituents (δ = ca. 9.6 ± 0.2 ppm) and computed NICS values at the center of the rings (NICS(0) = ca. –13 ± 1 ppm). This unique combination of structural, electrochemical, chromophoric, and magnetic features of the *carbo*-OPE backbone gives relevance to the prospect of synthesizing functional derivatives with donor and/or acceptor end groups that could operate as wire junctions, e.g., for SMC measurement. More generally any OPE-based molecular device would deserve comparison with the *carbo*-OPE counterpart.

6 Conclusions

This Account illustrates how proper extension of the structural variety for organic molecular materials relies on endeavors in the design and implementation of specific synthesis routes and methods. Indeed, while the highly versatile Sonogashira's *sp*^{2}C–*sp*C coupling procedure employed for the synthesis of alkynyl-benzenes is not applicable to alkynyl-*carbo*-benzene targets, the latter are readily accessible through the [6]pericyclynedione route, which proves to be definitely more efficient for alkynyl nucleophiles than for aryl and alkyl counterparts.[11c]

C_2-tethering of electroactive substituents to the C_{18} *carbo*-benzene ring is thus shown to be a subtle way to modulate functional properties while preserving a ‘soft’ *carbo*-aromatic character,[1b] featuring structural flexibility, visible optical absorptivity, electrical conductivity, and magnetic anisotropy. In the quadrupolar disubstituted series, a salient illustration is given for fluorenyl substituents: While insertion of C_2 connectors has a negligible effect on the OPA spectrum, it has a strong effect on the TPA spectrum. For 4-anilinyl substituents, the corresponding *carbo*-benzene **1o** exhibits an unprecedented single-molecule conductance, naturally anticipated to be lower for the C_2-expanded version **1p**. Nevertheless, the synthesis of **1p**, described here for the first time, allowed the finding of its remarkable surface aggregation and photosensitization ability securing the activity of a nanophotocatalytic system.[35] In the *carbo*-OPE series, the role of the C_2 linkers, ensuring conjugation between C_{18} rings while preserving their magnetic anisotropy, is to be highlighted for the development of new molecular wire systems.

More generally, it is noteworthy that the topological ‘aromatic character’ the C_2 tether (acetylene is the [2]annulene)[4f,10b] has a weaker insulating effect than the 1,4-phenylene tether: This can be interpreted by the weaker conformational dependence of the C_{18} functionality π-conjugation for the former.

The efficiency of the addition of alkynylmetals to [6]pericyclynediones also encourages further exploration of the C_2-tethering modulation approach. In particular, novel orientations beyond the quadrupolar series will be disclosed in due course.

Funding Information

The reported results have been obtained with fundings from the following sources: Agence Nationale de la Recherche (ANR-11-BS07-016-01), the Centre National de la Recherche Scientifique (CNRS pre-

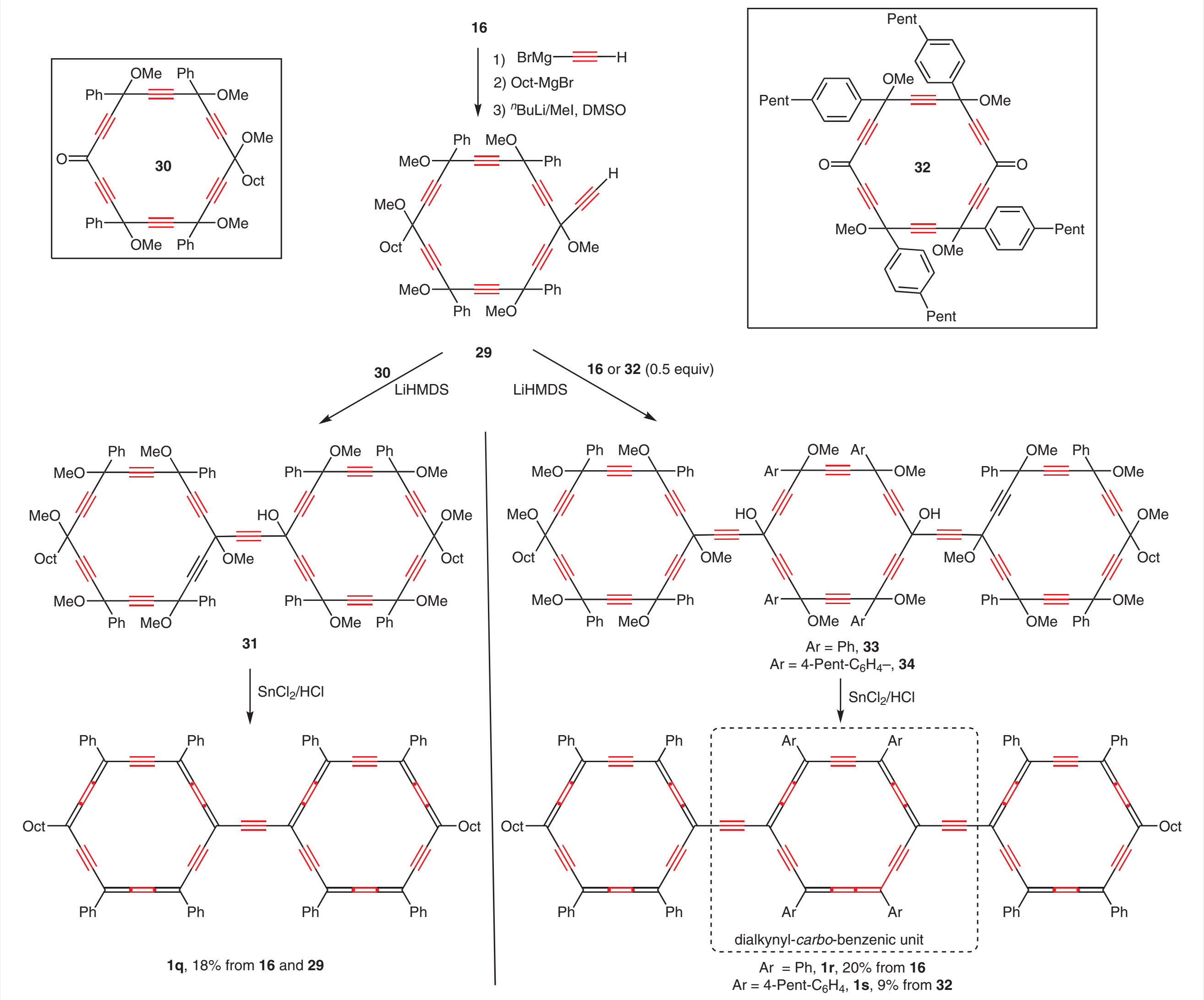

Scheme 8 Synthesis of the *carbo*-OPEs **1q** (*carbo*-biphenyl), **1r**, and **1s** (*carbo*-terphenyls)

maturation program, October 2016-November 2017, PHOTOH2 project), and the Toulouse IDEX program 2015-2017 (CARBO-DEVICE project).

Acknowledgment

The Centre National de la Recherche Scientifique (CNRS) is acknowledged for funding. K. C. and A. R. thank the Agence Nationale pour la Recherche (ANR) for their doctoral and post-doctoral fellowship, respectively. The authors are grateful to Alix Saquet for the electrochemical measurements and to all the co-authors of the cited references.

Supporting Information

DFT calculation data and comparative analysis of OPE[n] *vs* OPP[n] (ref. 2), INPUT and OUTPUT file extracts of DFT calculation of the dianilinyl derivatives **1o** and **1p**. Supporting information for this article is available online at https://doi.org/10.1055/s-0037-1610269.

References and Notes

(1) For reviews on *carbo*-mers see: (a) Maraval, V.; Chauvin, R. *Chem. Rev.* **2006**, *106*, 5317. (b) Cocq, K.; Lepetit, C.; Maraval, V.; Chauvin, R. *Chem. Soc. Rev.* **2015**, *44*, 6535. For the early definition, see: (c) Chauvin, R. *Tetrahedron Lett.* **1995**, *36*, 397. For references invoking the ethynylogation process, see: (d) Hafner, K.; Neuenschwander, M. *Angew. Chem., Int. Ed. Engl.* **1968**, *7*, 459. (e) Arnold, D. P.; James, D. A. *J. Org. Chem.* **1997**, *62*, 3460. (f) Young, B. S.; Herges, R.; Haley, M. M. *Chem. Commun.* **2012**,

9441. (g) Haley, M. M.; Chase, D. T.; Rose, B.; Fix, A. G. US9099660, **2015**. (h) Listunov, D.; Saffon-Merceron, N.; Joly, E.; Fabing, I.; Genisson, Y.; Maraval, V.; Chauvin, R. *Tetrahedron* **2016**, *72*, 6697.

(2) (a) A computational advance in this direction has been undertaken by comparison of ethynylogous OPE[n] and OPP[n], for n = 0–10. For a given π-conjugation extent n_C (= 6n + 6 for OPP[n], 8n + 6 for OPE[n]), the HOMO–LUMO gap is found always greater for OPE[(n_C–6)/8] than for OPP[(n_C–6)/6], becoming greater than 3.2 eV for $n_C \geq 54$ (corresponding to OPP[8] and OPE[6]). The OPE series is therefore definitely softer than the OPP series *vs* n_C. Calculations for ideal conjugation (under D_{2h} symmetry constraint) performed at the B3PW91/6-31G(d,p) level with the program Firefly 8.1.1: Granovsky, A. A. *Firefly Version 8* http://classic.chem.msu.su/gran/firefly/index.html) which is partially based on the GAMESS (US) source code. (b) Schmidt, M. W.; Baldridge, K. K.; Boatz, J. A.; Elbert, S. T.; Gordon, M. S.; Jensen, J. H.; Koseki, S.; Matsunaga, N.; Nguyen, K. A.; Su, S.; Windus, T. L.; Dupuis, M.; Montgomery, J. A. *J. Comput. Chem.* **1993**, *14*, 1347; see Supporting Information.

(3) (a) Kuwatani, Y.; Watanabe, N.; Ueda, I. *Tetrahedron Lett.* **1995**, *36*, 119. (b) Suzuki, R.; Tsukuda, H.; Watanabe, N.; Kuwatani, Y.; Ueda, I. *Tetrahedron* **1998**, *54*, 2477.

(4) For theoretical studies of *carbo*-mers, see for example: (a) Godard, C.; Lepetit, C.; Chauvin, R. *Chem. Commun.* **2000**, 1833. (b) Lepetit, C.; Godard, C.; Chauvin, R. *New J. Chem.* **2001**, *25*, 572. (c) Ducere, J.-M.; Lepetit, C.; Lacroix, P. G.; Heully, J.-L.; Chauvin, R. *Chem. Mater.* **2002**, *14*, 3332. (d) Lepetit, C.; Zou, C.; Chauvin, R. *J. Org. Chem.* **2006**, *71*, 6317. (e) Soncini, A.; Fowler, P. W.; Lepetit, C.; Chauvin, R. *Phys. Chem. Chem. Phys.* **2008**, *10*, 957. (f) Chauvin, R.; Lepetit, C.; Maraval, V.; Leroyer, L. *Pure Appl. Chem.* **2010**, *82*, 769. (g) Wodrich, M. D.; Gonthier, J. F.; Steinmann, S. N.; Corminboeuf, C. *J. Phys. Chem. A* **2010**, *114*, 6705. (h) Aspiroz, J. M.; Islas, R.; Moreno, D.; Fernández-Herrera, M. A.; Pan, S.; Chattaraj, P. K.; Martínez-Guajardo, G.; Ugalde, J. M.; Merino, G. *J. Org. Chem.* **2014**, *79*, 5463. (i) Poidevin, C.; Malrieu, J.-P.; Trinquier, G.; Lepetit, C.; Allouti, F.; Alikhani, M. E.; Chauvin, R. *Chem. Eur. J.* **2016**, *22*, 5295.

(5) (a) Rives, A.; Baglai, I.; Malytskyi, V.; Maraval, V.; Saffon-Merceron, N.; Voitenko, Z.; Chauvin, R. *Chem. Commun.* **2012**, *48*, 8763. (b) Rives, A.; Maraval, V.; Saffon-Merceron, N.; Chauvin, R. *Chem. Eur. J.* **2012**, *18*, 14702. (c) Rives, A.; Maraval, V.; Saffon-Merceron, N.; Chauvin, R. *Chem. Eur. J.* **2014**, *20*, 483.

(6) (a) Barthes, C.; Rives, A.; Maraval, V.; Chelain, E.; Brigaud, T.; Chauvin, R. *Fr.-Ukr. J. Chem.* **2015**, *3*, 60. (b) Rives, A.; Baglai, I.; Barthes, C.; Maraval, V.; Saffon-Merceron, N.; Saquet, A.; Voitenko, Z.; Volovenko, Y.; Chauvin, R. *Chem. Sci.* **2015**, *6*, 1139.

(7) Cocq, K.; Maraval, V.; Saffon-Merceron, N.; Saquet, A.; Poidevin, C.; Lepetit, C.; Chauvin, R. *Angew. Chem. Int. Ed.* **2015**, *54*, 2703.

(8) For references on [N]pericyclynes, see: (a) Scott, L. T.; DeCicco, G. J.; Hyun, J. L.; Reinhardt, G. *J. Am. Chem. Soc.* **1983**, *105*, 7760. (b) Scott, L. T.; DeCicco, G. J.; Hyun, J. L.; Reinhardt, G. *J. Am. Chem. Soc.* **1985**, *107*, 6546. For references on hexaoxy[6]pericyclynes, see: (c) Maurette, L.; Tedeschi, E.; Sermot, E.; Soleilhavoup, M.; Hussain, F.; Donnadieu, B.; Chauvin, R. *Tetrahedron* **2004**, *60*, 10077. (d) Leroyer, L.; Zou, C.; Maraval, V.; Chauvin, R. *C. R. Chimie* **2009**, *12*, 412.

(9) Chauvin, R. *Tetrahedron Lett.* **1995**, *36*, 401.

(10) (a) Saccavini, C.; Sui-Seng, C.; Maurette, L.; Lepetit, C.; Soula, S.; Zou, C.; Donnadieu, B.; Chauvin, R. *Chem. Eur. J.* **2007**, *13*, 4914. (b) Cocq, K.; Maraval, V.; Saffon-Merceron, N.; Chauvin, R. *Chem. Rec.* **2015**, *15*, 347.

(11) (a) Cocq, K.; Saffon-Merceron, N.; Poater, A.; Maraval, V.; Chauvin, R. *Synlett* **2016**, *27*, 2105. (b) Zhu, C.; Duhayon, C.; Saquet, A.; Maraval, V.; Chauvin, R. *Can. J. Chem.* **2017**, *95*, 454. (c) Zhu, C.; Rives, A.; Duhayon, C.; Maraval, V.; Chauvin, R. *J. Org. Chem.* **2017**, *82*, 925. (d) Listunov, D.; Duhayon, C.; Poater, A.; Mazères, S.; Saquet, A.; Maraval, V.; Chauvin, R. *Chem. Eur. J.* **2018**, *24*, 10699.

(12) (a) Lepetit, C.; Zou, C.; Chauvin, R. *J. Org. Chem.* **2006**, *71*, 6317. (b) Zou, C.; Duhayon, C.; Maraval, V.; Chauvin, R. *Angew. Chem. Int. Ed.* **2007**, *46*, 4337.

(13) For n = 6, see: (a) Diercks, D.; Armstrong, J. C.; Boese, R.; Vollhardt, K. P. C. *Angew. Chem., Int. Ed. Engl.* **1986**, *25*, 268. (b) Neena, T. X.; Whitesides, G. M. *J. Org. Chem.* **1988**, *53*, 2489. (c) Boese, R.; Green, J. R.; Mittendorf, J.; Mohler, D. L.; Vollhardt, K. P. C. *Angew. Chem., Int. Ed. Engl.* **1992**, *31*, 1643. (d) Haley, M. M. *Pure Appl. Chem.* **2008**, *80*, 519. (e) Jia, Z.; Li, Y.; Zuao, Z.; Liu, H.; Huang, C.; Li, Y. *Acc. Chem. Res.* **2017**, *50*, 2470. For n = 5, see: (f) Bunz, U. H. F.; Enkelmann, V.; Rader, J. *Organometallics* **1993**, *12*, 4745. (g) Jux, N.; Holczer, K.; Rubin, Y. *Angew. Chem., Int. Ed. Engl.* **1996**, *35*, 1986. (h) Steffen, W.; Laskoski, M.; Morton, J. G. M.; Bunz, U. H. F. *J. Organomet. Chem.* **2004**, *689*, 4345. For n = 4, see: (i) Bunz, U. H. F.; Enkelmann, V. *Angew. Chem., Int. Ed. Engl.* **1993**, *32*, 1653. (j) Laskoski, M.; Morton, J. G. M.; Smith, M. D.; Bunz, U. H. F. *J. Organomet. Chem.* **2002**, *652*, 21. (k) Esselman, B. J.; McMahon, R. J. *J. Phys. Chem. A* **2012**, *116*, 483. (l) Thompson, S. J.; Lee Emmert, F. III; Slipchenko, L. V. *J. Phys. Chem. A* **2012**, *116*, 3194. (m) Burgun, A.; Gendron, F.; Schauer, P. A.; Skelton, B. W.; Low, P. J.; Costuas, K.; Halet, J.-F.; Bruce, B.; Lapinte, C. *Organometallics* **2013**, *32*, 5015. For n = 4 and 8, see: (n) Yavari, I.; Jabbari, A.; Samadizadeh, M. *J. Chem. Res., Synop.* **1999**, 152. For n = 3, see: (o) Domnin, I. N.; Takhistov, V. V.; Ponomarev, D. A. *Eur. Mass Spectrom.* **1999**, *5*, 169. (p) Morton, M. S.; Selegue, J. P. *J. Organomet. Chem.* **1999**, *578*, 133.

(14) Basic calculations of the heterolytic bond dissociation energy ΔE(R), corresponding to the equation $(\mathrm{MeC{\equiv}C})_2\mathrm{RC{-}OH} \rightarrow (\mathrm{MeC{\equiv}C})_2\mathrm{RC}^+ + \mathrm{OH}^-$ in the gas phase, show that $\Delta E(\mathrm{MeC{\equiv}C}) - \Delta E(\mathrm{Ph}) = +3$ kcal/mol: $\Delta E(\mathrm{MeC{\equiv}C}) = 0.32935$ Ha, $\Delta E(\mathrm{Ph}) = 0.32458$ Ha, $\Delta E(\mathrm{Me}) = 0.34930$ Ha, $\Delta E(\mathrm{H}) = 0.36285$ Ha. Calculations at the B3PW91/6-31G(d,p) level with the program Firefly 8.1.1: see ref. 2a,b.

(15) (a) Nicholas, K. M. *Acc. Chem. Res.* **1987**, *20*, 207. (b) McGlinchey, M. J.; Girard, L.; Ruffolo, R. *Coord. Chem. Rev.* **1995**, *143*, 331. (c) Melikyan, G. G.; Bright, S.; Monroe, T.; Hardcastle, K. I.; Ciurash, J. *Angew. Chem. Int. Ed.* **1998**, *37*, 161.

(16) Karadakov, P. B. *Chem. Phys. Lett.* **2016**, *646*, 190.

(17) Cocq, K.; Saffon-Merceron, N.; Coppel, Y.; Poidevin, C.; Maraval, V.; Chauvin, R. *Angew. Chem. Int. Ed.* **2016**, *55*, 15133.

(18) Saccavini, C.; Tedeschi, C.; Maurette, L.; Sui-Seng, C.; Zou, C.; Soleilhavoup, M.; Vendier, L.; Chauvin, R. *Chem. Eur. J.* **2007**, *13*, 4895.

(19) For the preparation of dibenzoylacetylene **12**, see: Zhang, Z. Z.; Schuster, G. B. *J. Am. Chem. Soc.* **1989**, *111*, 7149.

(20) (a) Hrobárik, P.; Hrobáriková, V.; Semak, V.; Kasák, P.; Rakovský, E.; Polyzos, I.; Fakis, M.; Persephonis, P. *Org. Lett.* **2014**, *16*, 6358. (b) Tran, C.; Berqouch, N.; Dhimane, H.; Clermont, G.; Blanchard-Desce, M.; Ogden, D.; Dalko, P. I. *Chem. Eur. J.* **2017**, *23*, 1860.

(21) Belfield, K. D.; Yao, S.; Bondar, M. V. *Adv. Polym. Sci.* **2008**, *213*, 97.

(22) Baglai, I.; de Anda-Villa, M.; Barba-Barba, R. M.; Poidevin, C.; Ramos-Ortíz, G.; Maraval, V.; Lepetit, C.; Saffon-Merceron, N.; Maldonado, J.-L.; Chauvin, R. *Chem. Eur. J.* **2015**, *21*, 14186.

(23) For a recent review on discotic liquid crystals, see: Wöhrle, T.; Wurzbach, I.; Kirres, J.; Kostidou, A.; Kapernaum, N.; Litterscheidt, J.; Haenle, J. C.; Staffeld, P.; Baro, A.; Giesselmann, F.; Laschat, S. *Chem. Rev.* **2016**, *116*, 1139.

(24) Rives, A.; Maraval, V.; Chauvin, R. *unpublished results*.

(25) Zhu, C.; Wang, T.-H.; Su, C.-J.; Lee, S.-L.; Rives, A.; Duhayon, C.; Kauffmann, B.; Maraval, V.; Chen, C.-h.; Hsu, H.-F.; Chauvin, R. *Chem. Commun.* **2017**, *53*, 5902.

(26) Wu, J.; Warson, M. D.; Zhang, L.; Wang, Z.; Müllen, K. *J. Am. Chem. Soc.* **2004**, *126*, 177.

(27) Rives, A.; Baglai, I.; Malytskyi, V.; Maraval, V.; Saffon-Merceron, N.; Voitenko, Z.; Chauvin, R. *Chem. Commun.* **2012**, *48*, 8763.

(28) Baglai, I.; Maraval, V.; Bijani, C.; Saffon-Merceron, N.; Voitenko, Z.; Volovenko, Y. M.; Chauvin, R. *Chem. Commun.* **2013**, *49*, 8374.

(29) Baglai, I.; Maraval, V.; Duhayon, C.; Chauvin, R. *Acta Crystallogr., Sect. E: Struct. Rep. Online* **2013**, *69*, o921.

(30) (a) Bhattacharya, A.; Vasques, T.; Ramirez, T.; Plata, R. E.; Wu, J. *Tetrahedron Lett.* **2006**, *47*, 5581. (b) Nemoto, H.; Fujita, S.; Nagai, M.; Fukumoto, K.; Kametani, T. *J. Am. Chem. Soc.* **1988**, *110*, 2931.

(31) **Experimental Procedure and Characterization of 27b**

First Step

Bis(benzonitrile)palladium(II)chloride (41.3 mg, 0.107 mmol) and CuI (9.6 mg, 0.074 mmol) were placed into a Schlenk tube under argon and dissolved in 4 mL of dry 1,4-dioxane. The mixture was then treated with tri-*tert*-butylphosphine (0.22 mL, 1 M solution in toluene, 0.22 mmol) at r.t. After the solution turned black, distilled diisopropylamine (0.65 mL, 4.99 mmol), 4-bromo-*N*,*N*-bis(trimethylsilyl)aniline (1.0 mL, 3.54 mmol) and trimethylsilylacetylene (0.65 mL, 4.60 mmol) were added. The resulting mixture was heated at 50 °C for 2 h, and then cooled down to r.t. before addition of EtOAc, filtering through Celite®, and concentration under reduced pressure to afford **29** as a black sticky liquid (1.42 g), which was used without further purification.

Second Step

A solution of the crude product **29** (1.42 g) in methanol (20 mL) was cooled down to 0 °C, before treatment with K_2CO_3 (884 mg, 6.40 mmol). The resulting mixture was stirred for 1 h at 0 °C before addition of distilled water (20 mL). Then, the methanol was removed under reduced pressure. The remaining aqueous layer was extracted with Et_2O, and the combined organic layers were washed with brine, dried over anhydrous $MgSO_4$, and concentrated under reduced pressure to afford **27b** as a spectroscopically pure brown viscous liquid (920 mg, 3.50 mmol, 98% yield over 2 steps).

Analytical Data

^{1}H NMR (400 MHz, 298 K, $(CD_3)_2CO$): δ = 0.10 (s, 18 H, -Si$(CH_3)_3$), 3.7 (s, 1 H, ≡CH) 6.96 (d, $^3J_{HH}$ = 8.0 Hz, 2 H, *o*-C_6H_4–), 7.39 (d, $^3J_{HH}$ = 8.0 Hz, 2 H, *m*-C_6H_4–) ppm. ^{13}C{^{1}H} NMR (100 MHz, 298 K, $(CD_3)_2CO$): δ = 1 .31 (–Si$(CH_3)_3$), 77.66 (–C≡*C*–H), 83.37 (–*C*≡C–H), 117.54 (*ipso*-C_6H_4), 130.28 (*o*-C_6H_4), 132.77 (*m*-C_6H_4), 149.08 (*p*-C_6H_4) ppm.

(32) **Experimental Preparation and Characterization of 1p**

First Step

A solution of **27b** (638 mg, 2 .44 mmol) in dry THF (15 mL) was treated at –78 °C with lithium bis(trimethylsilyl)amide (2.8 mL, 1 M solution in THF, 2.8 mmol). The resulting mixture was stirred for 1 h at –78 °C before dropwise addition of a solution of **16** (706 mg, 1.04 mmol) in dry THF (60 mL) at the same temperature. The resulting mixture was allowed to warm up to r.t. under stirring over 18 h. After treatment with a saturated aqueous solution of NH_4Cl and extractions of the aqueous layer with Et_2O, the combined organic layers were washed with brine, dried over anhydrous $MgSO_4$, and concentrated under reduced pressure to afford the diol **28b** as an orange solid (1.48 g), which was used without further purification.

Second Step

A solution of the crude **28b** (1.48 g) in dry DCM (330 mL) was treated at –78 °C with $SnCl_2$ (2.43 g, 12.8 mmol) and HCl·Et_2O (12.4 mL, 2 M solution in Et_2O, 24.8 mmol). The resulting mixture was allowed to warm up to –15 °C under stirring over 3.5 h, and then kept for 10 min. at r.t. before addition of NaOH (25 mL, 2 M aqueous solution, 50 mmol). The resulting mixture was stirred at r.t. for 16 h. After treatment with a saturated aqueous solution of Na_2CO_3 and extractions of the aqueous layer with DCM, the combined organic layers were dried over anhydrous $MgSO_4$ before filtration through Celite® and concentration under reduced pressure. Washings of the crude solid with pentane and Et_2O afforded the expected *carbo*-benzene **1p** as a dark violet solid (160 mg, 0.21 mmol, 20% yield over 2 steps).

Analytical Data

^{1}H NMR (400 MHz, 298 K, (D_8-THF)): δ = 5.38 (br s, 4 H, –NH_2), 6.83 ($^3J_{HH}$ = 8.0 Hz, 4 H, *m*-C_6H_4–NH_2), 7.70 (t, $^3J_{HH}$ = 8.0 Hz, 4 H, *p*-C_6H_5), 7,80 (d, $^3J_{HH}$ = 8.0 Hz, 4 H, *o*-C_6H_4–NH_2), 7.98 (t, $^3J_{HH}$ = 8.0 Hz, 8 H, *m*-C_6H_5), 9.47 (t, $^3J_{HH}$ = 8.0 Hz, 8 H, *o*-C_6H_5) ppm. ^{13}C{^{1}H} NMR (100 MHz, 298 K, (D_8-THF)): δ = 87.00–113.90 (–C≡C– and >C≡C=C≡C<), 115,16 (m-C_6H_4–NH_2), 119,85, 120,81 (>*C*(C_6H_4–NH_2)– and >*C*(C_6H_5)–), 130.00–130.84 (*o*, *m*, *p*-C_6H_5), 134.85 (*o*-C_6H_4–NH_2), 140.33, 152.07 (*p*-C_6H_4–NH_2 and *p*-C_6H_5) ppm. MS (MALDI-TOF/DCTB): *m*/*z* (%) = 756.2 (100) [M]$^+$.HRMS (MALDI-TOF/DCTB): *m*/*z* [M]$^+$ calcd for $C_{58}H_{32}N_2$: 756.2565; found: 756.2602; [M + Na]$^+$ calcd for $C_{58}H_{32}N_2Na$: 779.2463; found: 779.2437. UV-vis (THF): $\lambda_{max}(\varepsilon)$ = 493 nm (131000 L/mol/cm). Voltammetry: reduction: *E* (V/SCE) = –0.67 (rev), –1.09 (rev), –1.56 (irrev), oxidation: 0.74 (irrev).

(33) (a) Li, Z.; Smeu, M.; Rives, A.; Maraval, V.; Chauvin, R.; Ratner, M. A.; Borguet, E. *Nature Commun.* **2015**, 6, 6321. For the STM-break junction method, see: (b) Xu, B. Q.; Tao, N. J. *Science* **2003**, *301*, 1221.

(34) Choi, S. H.; Kim, B. S.; Frisbie, C. D. *Science* **2008**, *320*, 1482.

(35) (a) Cure, J.; Kahn, M.; Cocq, K.; Casterou, G.; Chauvin, R.; Maraval, V. FR 1660040, **2016**. (b) Cure, J.; Kahn, M.; Cocq, K.; Casterou, G.; Chauvin, R.; Maraval, V.; Assi, H. PCT/FR 2017/052842, **2017**.

(36) Zhu, C.; Poater, A.; Duhayon, C.; Kauffmann, B.; Saquet, A.; Maraval, V.; Chauvin, R. *Angew. Chem. Int. Ed.* **2018**, *57*, 5640.

(37) See for example: (a) Lu, Q.; Yao, C.; Wang, X.; Wang, F. *J. Phys. Chem. C* **2012**, *116*, 17853. (b) Parker, C. R.; Leary, E.; Frisenda, R.; Wei, Z.; Jennum, K. S.; Glibstrup, E.; Abrahamsen, P. B.; Santella, M.; Christensen, M. A.; Della Pia, E. A.; Li, T.; Gonzalez, M. T.; Jiang, X.; Morsing, T. J.; Rubio-Bollinger, G.; Laursen, B. W.; Nørgaard, K.; van der Zant, H.; Agrait, N.; Brønsted, Nielsen. M. *J. Am. Chem. Soc.* **2014**, *136*, 16497.